Determination of the Role of Target Tissue Metabolism in Lung Carcinogenesis Using Conditional Cytochrome *P*450 Reductase-Null Mice

Yan Weng, Cheng Fang, Robert J. Turesky, Melissa Behr, Laurence S. Kaminsky, and Xinxin Ding

Wadsworth Center, New York State Department of Health, and School of Public Health, State University of New York at Albany, Albany, New York

Abstract

Critical to mechanisms of chemical carcinogenesis and the design of chemopreventive strategies is whether procarcinogen bioactivation in an extrahepatic target tissue (e.g., the lung) is essential for tumor formation. This study aims to develop a mouse model capable of revealing the role of pulmonary microsomal cytochrome P450 (P450)–mediated metabolic activation in xenobiotic-induced lung cancer. A novel triple transgenic mouse model, with the NADPH-P450 reductase (*Cpr*) gene deleted in a lung-specific and doxycycline-inducible fashion (lung-*Cpr*-null), was generated. CPR, the obligate electron donor for microsomal P450 enzymes, is essential for the bioactivation of many procarcinogens. The lung-*Cpr*-null mouse was studied to resolve whether pulmonary P450 plays a major role in 4-(methylnitrosamino)-1–(3-pyridyl)-1-butanone (NNK)–induced lung cancer by producing carcinogenic metabolites in the target tissue. A liver-*Cpr*-null mouse was also studied to test whether hepatic P450 contributes predominantly to systemic clearance of NNK, thereby decreasing NNK-induced lung cancer. The numbers of NNK-induced lung tumors were reduced in the lung-*Cpr*-null mice but were increased in the liver-*Cpr*-null mice, relative to wild-type control mice. Decreased lung tumor multiplicity in the lung-*Cpr*-null mice correlated with reduced lung O^6-methylguanine adduct levels, without decreases in NNK bioavailability, consistent with decreased NNK bioactivation in the lung. Moreover, lung tumors in lung-*Cpr*-null mice were positive for CPR expression, indicating that the tumors did not originate from *Cpr*-null cells. Thus, we have confirmed the essential role of pulmonary P450-mediated metabolic activation in NNK-induced lung cancer, and our mouse models should be applicable to studies on other procarcinogens that require P450-mediated metabolic activation. [Cancer Res 2007;67(16):7825–32]

Introduction

Microsomal cytochrome P450 (P450) enzymes catalyze the metabolism of various endogenous and exogenous compounds (1). In many cases, P450-mediated metabolic activation of a xenobiotic compound is a key step that leads to acute toxicity or carcinogenicity. At the organ level, P450 enzymes are most abundant in the liver, and hepatic P450-mediated metabolic activation is often the major contributor to xenobiotic-induced hepatotoxicity (e.g., ref. 2). However, for most chemical compounds, it is not known whether hepatic P450-mediated metabolic activation is also responsible for chemical-induced toxicity and carcinogenicity in extrahepatic organs, such as the lung.

The lung is a portal-of-entry organ for airborne environmental compounds. The expression of many microsomal P450s has been detected in human lung (3), as well as in lungs of laboratory animals (4). Pulmonary P450-mediated metabolic activities may play important roles in environmental chemical-induced toxicities (3). However, metabolites generated in the liver or elsewhere may also reach the lung to cause toxicity, as shown by our recent finding that acetaminophen toxicity in mouse lung was at least partially dependent on metabolic activation in the liver (2). Because of the lack of appropriate experimental approaches, direct evidence for the role of pulmonary P450-mediated metabolic activation in xenobiotic-induced lung toxicity and carcinogenicity is still lacking for most, if not all, xenobiotic compounds.

The microsomal P450 system consists of P450 enzymes and their electron donor, NADPH-P450 reductase (CPR). In contrast to the multiplicity of *CYP* genes, there is only one *Cpr* gene in mammals (5), a fact which makes it feasible to knock out the activities of all microsomal P450 enzymes via the deletion of this single *Cpr* gene. Germ-line deletion of *Cpr* is embryonically lethal in mice (6, 7). However, mouse models with liver-specific *Cpr* deletion (liver-*Cpr*-null) are viable (8, 9). In this study, a novel triple transgenic mouse model (lung-*Cpr*-null), which permits doxycycline-inducible, lung-specific *Cpr* deletion, was generated and used to test the role of pulmonary P450 in 4-(methylnitrosamino)-1-(3-pyridyl)-1-butanone (NNK)–induced lung carcinogenesis.

NNK is one of the most potent carcinogens identified in tobacco smoke. NNK can readily induce lung adenoma in laboratory animals (10) and is also considered a major risk factor for human lung adenocarcinoma, which is currently the most frequent lung cancer type (11). NNK-induced lung carcinogenesis is believed to occur via P450-mediated α-hydroxylation, which leads to production of reactive metabolites that induce the formation of DNA adducts, including O^6-methylguanine (O^6-mG; refs. 10, 12). The *in vivo* role of P450 in NNK-induced carcinogenesis has been indicated in studies using structurally diverse P450 inhibitors (10, 13–15). However, although P450 isoforms active toward NNK are expressed in the respiratory tract in rodents and humans (16, 17), liver microsomes are at least as active as lung microsomes in NNK metabolic activation *in vitro* (18), and there is no direct evidence regarding whether target tissue bioactivation is required for NNK-induced carcinogenesis. In the experiments using P450 inhibitors, where the inhibitors could interact with P450 enzymes throughout the body, it was not possible to distinguish

Note: Supplementary data for this article are available at Cancer Research Online (http://cancerres.aacrjournals.org/).

Requests for reprints: Xinxin Ding, Wadsworth Center, New York State Department of Health, Empire State Plaza, Box 509, Albany, NY 12201-0509. Phone: 518-486-2585; Fax: 518-486-1505; E-mail: xding@wadsworth.org.

doi:10.1158/0008-5472.CAN-07-1006

contributions from differing tissues or cells. A system that permits tissue- or cell-selective modulation of P450 function in the lung has not been available until now.

To study the relative contributions of pulmonary and hepatic microsomal P450 enzymes in NNK-induced lung carcinogenesis, we first back-crossed the lung-*Cpr*-null and liver-*Cpr*-null mice to the susceptible A/J strain (19). The conditional *Cpr*-null offspring and their littermate controls were then studied for NNK-induced lung tumor formation, O^6-mG formation in the lung and liver, and systemic clearance of NNK and its major metabolite 4-(methylnitrosamino)-1-(3-pyridyl)-1-butanol (NNAL). Our results strongly support the hypothesis that pulmonary P450 enzymes play an essential role in NNK-induced lung carcinogenesis by producing carcinogenic metabolites directly in the target tissue, whereas hepatic P450 enzymes play an important role in systemic clearance of NNK, thereby decreasing the bioavailability of NNK in the lung and the susceptibility to NNK-induced lung carcinogenesis.

Materials and Methods

Mouse breeding. The liver-*Cpr*-null (8) and $Cpr^{lox/lox}$ mice (transgenic mice with floxed *Cpr* alleles; ref. 20) were from breeding stocks maintained at the Wadsworth Center. The *CCSP-rtTA/tetO-Cre* mouse was a kind gift from Dr. Jeffery A. Whitsett of the University of Cincinnati (Cincinnati, OH; refs. 21–23). The lung-*Cpr*-null mice were generated by cross-breeding *CCSP-rtTA/tetO-Cre* mice and $Cpr^{lox/lox}$ mice. The *CCSP-rtTA/tetO-Cre* mice (on a mixed 129/Sv and FVB/N background) and the $Cpr^{lox/lox}$ mice (on a mixed C57BL/6 and 129/Sv background) were each backcrossed thrice to the A/J strain, before they were intercrossed to obtain the A/J-N_3 lung-*Cpr*-null mice ($CCSP\text{-}rtTA^{hemi}/tetO\text{-}Cre^{hemi}/Cpr^{lox/lox}$) and control littermates ($CCSP\text{-}rtTA^{hemi}/Cpr^{lox/lox}$ or $Cpr^{lox/lox}$; see Supplementary Fig. S1 for a detailed breeding scheme). The liver-*Cpr*-null mouse (on a mixed C57BL/6 and 129/Sv background) was backcrossed to the A/J strain five times, before the heterozygotes were intercrossed to obtain A/J-N_5 liver-*Cpr*-null ($Alb\text{-}Cre^{hemi}/Cpr^{lox/lox}$) and wild-type (WT; $Cpr^{lox/lox}$) littermates.

Animal use and doxycycline treatment. All animal use protocols were approved by the Institutional Animal Care and Use Committee of the Wadsworth Center. Mice not treated with doxycycline were fed with a standard chow diet (Prolab RMH350) *ad libitum*. For studies of doxycycline-induced *Cpr* deletion in the lung-*Cpr*-null mice, the animals were kept on doxycycline-containing food pellets (625 mg/kg; Harlan Teklad) either between the ages of 1 and 2 months or between E0 (through the dam) and the age of 2 months, according to a reported protocol (24). The amount of food consumed was ~3 g daily per mouse, at 6 weeks to 4 months of age.

NNK treatment. For pharmacokinetic studies and determination of tissue levels of O^6-mG, the animals were treated with NNK by a single i.p. injection at the dose of 100 mg/kg for the liver-*Cpr*-null mice and WT control littermates or 200 mg/kg or 20 μmol/mouse for the lung-*Cpr*-null mice and control littermates. Blood samples were collected by tail bleeding with a heparin-coated capillary at 5, 20, 60, 120, 240, and 480 min after NNK injection. Lungs and livers were collected for determination of tissue levels of O^6-mG at 4 or 24 h after NNK injection and stored at −80°C until use.

Lung tumor formation was induced with NNK according to the protocol of Jalas et al. (12). All animals, at the age of 2 months, with or without the doxycycline treatment from E0, were given a single i.p. injection of 0.15 mL of either saline or NNK at either 20 μmol/mouse for the lung-*Cpr*-null mice and control littermates or 10 μmol/mouse for the liver-*Cpr*-null mice and WT littermates. Following the injection, all animals were maintained on AIN-93G diet (Dyets, Inc.) until sacrificed 4 months later for the tumor bioassay. The lung tumor multiplicity (averaged number of tumors per mouse) and frequency (percentage of mice with tumors) were determined independently by two researchers, and the averages of the two analyses are reported.

Other methods. Pharmacokinetic variables were calculated using the WinNonlin software (version 5.0.1) from Pharsight. Methods for analysis of genotypes of the transgenic mice; immunohistochemical analysis of CPR, surfactant protein C (SP-C), and Clara cell secretary protein (CCSP) expression; quantitative PCR analysis of the abundance of the Cpr^- (deleted *Cpr* allele) and Cpr^{lox} alleles; quantitative PCR analysis of SP-C mRNA expression levels in the isolated alveolar type II cell preparations and in the whole lung; and determination of tissue levels of O^6-mG and plasma levels of NNK and NNAL are described in the Supplementary Data. Statistical analyses were done with use of the SigmaStat software (SPSS, Inc.). Statistical significance of differences between two groups in various variables was examined using Student's *t* test; for samples that failed

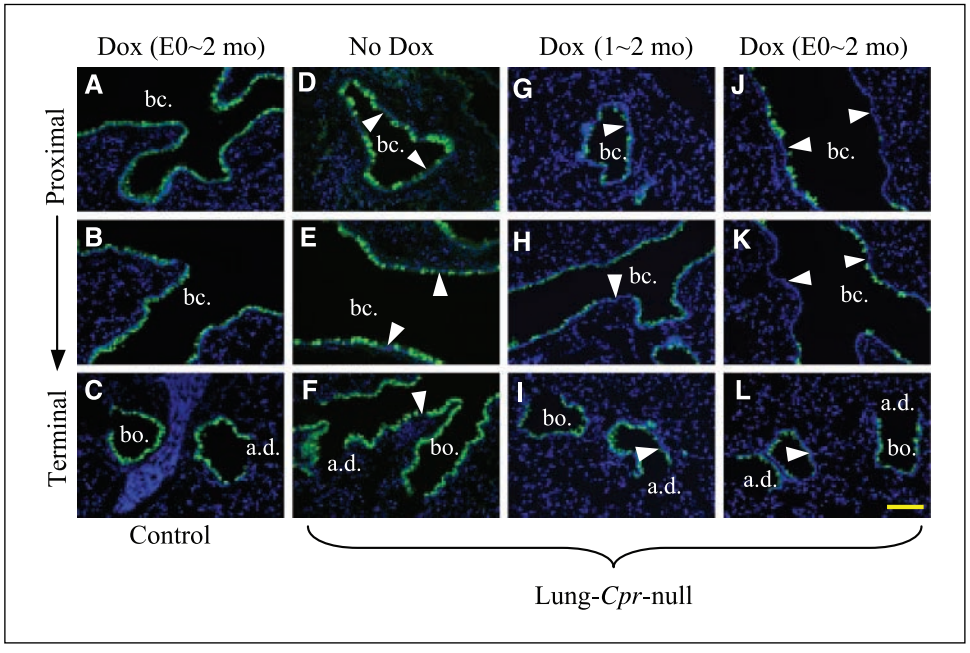

Figure 1. Immunohistochemical analysis of CPR expression in the lungs of untreated or doxycycline (*Dox*)-treated lung-*Cpr*-null mice and control littermates. Paraffin sections (4–5 μm) of lungs from 2-month-old female mice were analyzed with a rabbit anti-rat CPR antibody (*A–L*). Alexa Fluor 488–conjugated secondary antibody was used for visualization of the antigen sites. Regions corresponding to the proximal, midlevel, and terminal airways were included for each group. No signal was detected when the primary antibody was replaced by a normal goat serum (data not shown). Control littermates (*A–C*) were treated with doxycycline from E0. Lung-*Cpr*-null mice were either untreated (*D–F*) or treated with doxycycline from the age of 1 mo (*G–I*) or from E0 (*J–L*). The images were representative of at least three mice analyzed in each group. Bar, 50 μm. *Arrowheads,* examples of CPR-negative cells. *a.d.,* alveolar duct; *bc.,* bronchus; *bo.,* bronchiole.

Table 1. NNK-induced O^6-mG adduct formation and lung tumorigenesis in lung-*Cpr*-null mice and control littermates

A. Lung tumor multiplicity and frequency

Animals	Treatment	Tumor multiplicity (tumors/mouse)	Tumor frequency (%)
Control-Dox	Saline (n = 8)	0 ± 0	0
Control-Dox	NNK (n = 14)	34.4 ± 3.9*	100 †
Lung-*Cpr*-null-Dox	Saline (n = 6)	0.17 ± 0.17	17
Lung-*Cpr*-null-Dox	NNK (n = 12)	14.8 ± 3.1* ‡	92 †

B. Tissue levels of O^6-mG

Animals	O^6-mG (pmol/μmol guanine)		
	4 h	24 h	
	Lung	Lung	Liver
Control	26.5 ± 3.1	64.3 ± 9.8	370 ± 20
Control-Dox	35.1 ± 2.3 (n = 5)	67.7 ± 8.2	370 ± 30
Lung-*Cpr*-null-Dox	13.1 ± 0.4 (n = 3)§	30.9 ± 5.4§	390 ± 30

NOTE: A. All mice were female and were treated with doxycycline from E0. At 2 mo of age, they received a single i.p. injection of either NNK (20 μmol/mouse) or 0.15 mL saline. Thereafter, doxycycline treatment ceased, and all animals were kept on AIN93G diet until they were sacrificed for tumor bioassay, at 4 mo after the NNK or saline injection. Tumor multiplicity is shown as mean ± SE. Tumor frequency was calculated as percentage of mice with tumor in each group. Histologic characterization of these lung tumors (see Supplementary Data) indicated that they represent foci of hyperplasia or adenoma, but not carcinoma; lymphoid nodules and perivascular lymphoid cuffs were also seen, as evidence of subacute to chronic inflammation, which could be secondary to tumor growth. B. Animals (2-month-old females) were either given a single i.p. injection of NNK at 20 μmol/mouse and sacrificed at 4 h or given an i.p. dose of 200 mg/kg and sacrificed at 24 h after dosing. The values shown are mean ± SE (n = 4, unless specified otherwise). Examples of the detection of pulmonary O^6-mG are shown in Supplementary Fig. S3.

Abbreviation: Dox, doxycycline.

*Significantly different from corresponding saline-treated groups (P < 0.01, Mann-Whitney rank-sum test).

†Significantly different from corresponding saline-treated groups (P < 0.01, Fisher's exact test).

‡Significantly different from NNK-treated control-doxycycline group (P < 0.001, t test).

§Significantly different from control-doxycycline mice in the same column (P < 0.05, t test).

normality test, Mann-Whitney rank-sum test was used instead. Statistical significance of differences in tumor frequency was analyzed using Fisher's exact test.

Results

General characterization of the lung-*Cpr*-null mice. The lung-*Cpr*-null (*CCSP-rtTA*^{hemi}/*tetO-Cre*^{hemi}/*Cpr*$^{lox/lox}$) mouse was prepared by cross-breeding *CCSP-rtTA/tetO-Cre* mice (21–23) and *Cpr*$^{lox/lox}$ mice (20). In these mice, the expression of Cre recombinase is controlled by the tetracycline operator (tetO), which can be activated by the reverse tetracycline transactivator (rtTA) in the presence of doxycycline. The rtTA transgene is driven by the rat CCSP promoter, which is active in the Clara cells in the airway and type II epithelial cells in the alveoli of the transgenic mice (21, 23, 25).

The A/J-N_3 lung-*Cpr*-null mice and control littermates, containing ~88% of the recipient A/J genetic background (26), were used for characterization and subsequent metabolism and toxicology studies. The lung-*Cpr*-null mice were normal compared with the control littermates. There was no indication of embryonic lethality associated with the lung-*Cpr*-null genotype (Supplementary Table S1). No behavioral changes were noticed. There was no significant difference in either body weight or weights of lung and liver, between adult female lung-*Cpr*-null mice and control littermates at the age of 2 months, for either untreated mice (data not shown) or mice treated with doxycycline (Supplementary Table S2). Body and organ weights were not determined for the male mice. No histologic changes were observed in the lungs of the lung-*Cpr*-null mice, either with or without doxycycline treatment (e.g., see Supplementary Fig. S2).

Doxycycline-induced *Cpr* deletion in the lungs of the lung-*Cpr*-null mice. CPR was detected in virtually all epithelial cells lining the conducting airway in the control mice (data not shown), and this expression pattern was not altered by doxycycline treatment (Fig. 1*A–C*), indicating that doxycycline treatment did not have any noticeable effect on CPR expression. In untreated lung-*Cpr*-null mice, the loss of CPR expression was observed in a small fraction of the airway epithelial cells (Fig. 1*D–F*), presumably due to the "leakiness" of the *tetO-Cre* transgene expression (23, 25). However, the number of cells lacking CPR expression was clearly much greater in doxycycline-treated lung-*Cpr*-null mice (Fig. 1*G–L*) than in the untreated ones (Fig. 1*D–F*). Furthermore, in untreated lung-*Cpr*-null mice (Fig. 1*D–F*) or in lung-*Cpr*-null mice treated with doxycycline between ages of 1 to 2 months (Fig. 1*G–I*), the CPR-negative cells were randomly distributed around the airway, whereas in the lung-*Cpr*-null mice treated with doxycycline between E0 and the age of 2 months, the CPR-negative cells

appeared in large patches, resulting in long stretches of CPR-negative cells, usually present on only one side of the airway (Fig. 1*J–L*).

The extent of *Cpr* deletion in the alveolar type II epithelial cells (AECII) was determined using quantitative DNA-PCR in AECII cell preparations (~2.5-fold enriched, compared with the whole lung) from 2-month-old lung-*Cpr*-null mice (Supplementary Table S3). The extents of *Cpr* deletion in the AECII-enriched cell preparations, which should still be lower than the extents in a pure AECII cell preparation, were significantly higher than those in the whole lung in either untreated (17.4% in AECII versus 6.2% in whole lung) or doxycycline-treated lung-*Cpr*-null mice (32.2% in AECII versus 18.2% in whole lung), indicating that *Cpr* was preferentially deleted in this cell type. The E0- to 2-month doxycycline treatment protocol, which was more effective than the 1- to 2-month doxycycline treatment protocol for induction of *Cpr* deletion (Fig. 1*G–I* versus *J–L*; Supplementary Table S3), was used for all subsequent studies. In the following text, we will use "lung-*Cpr*-null-doxycycline" and "control-doxycycline" to represent lung-*Cpr*-null and control littermates, respectively, treated with doxycycline between E0 and the age of 2 months.

NNK-induced lung tumor formation in the lung-*Cpr*-null mice and control littermates. The effects of *Cpr* deletion in the lung on NNK-induced lung tumor formation were determined using the lung-*Cpr*-null-doxycycline and control-doxycycline mice, and the results are shown in Table 1A. Female mice were used for these and subsequent studies because the NNK tumor bioassay was originally established using female mice, which are more sensitive than male mice to NNK-induced lung tumor formation (27). Following a single i.p. injection of NNK at 20 μmol/mouse, lung tumor multiplicity in the lung-*Cpr*-null-doxycycline mice (14.8 tumors per mouse) was ~43.0% of that in similarly treated control-doxycycline mice (34.4 tumors per mouse). Within the NNK-treated control-doxycycline group, there was no difference in lung tumor multiplicity between *CCSP-rtTA/Cpr*$^{lox/lox}$ mice (34.6 tumors per mouse, n = 8) and *Cpr*$^{lox/lox}$ mice (34.2 tumors per mouse, n = 6). No tumor was detected in saline-treated control-doxycycline mice, and only one of six saline-treated lung-*Cpr*-null-doxycycline mice had a single lung tumor. There was no significant difference in tumor frequency between NNK-treated control-doxycycline (100%) and NNK-treated lung-*Cpr*-null-doxycycline mice (92%) or between saline-treated control-doxycycline (0%) and saline-treated lung-*Cpr*-null-doxycycline mice (17%). The averaged body weight at either 2 months of age (Supplementary Table S2) or at the time of tumor bioassay (Table 1A) did not differ significantly among the groups studied. NNK-induced tumors were not detected in other organs examined, including liver, heart, pancreas, kidney, uterus, brain, and nose (data not shown). In other experiments not presented, doxycycline treatment was found to not affect lung tumor multiplicity in NNK-treated WT A/J mice.

Tumors in the NNK-treated lung-*Cpr*-null mice were derived from CPR-expressing AECII cells. The NNK-induced adenoma or adenocarcinoma in the lungs of the A/J mice is believed to originate primarily from AECII cells (28). However, NNK-induced lung tumors have also been reported to originate from Clara cells (29). Because *Cpr* deletion occurred in only a portion of the Clara cells and AECII cells in the lung-*Cpr*-null mice, the residual lung tumors could have originated from Clara and/or AECII cells that have an intact *Cpr* and thus normal CPR expression or from other types of lung cells, which also have an intact *Cpr*. Therefore, we examined the expressions of CPR, SP-C (a marker of AECII cells), and CCSP (a marker of Clara cells) in 48 tumors from three

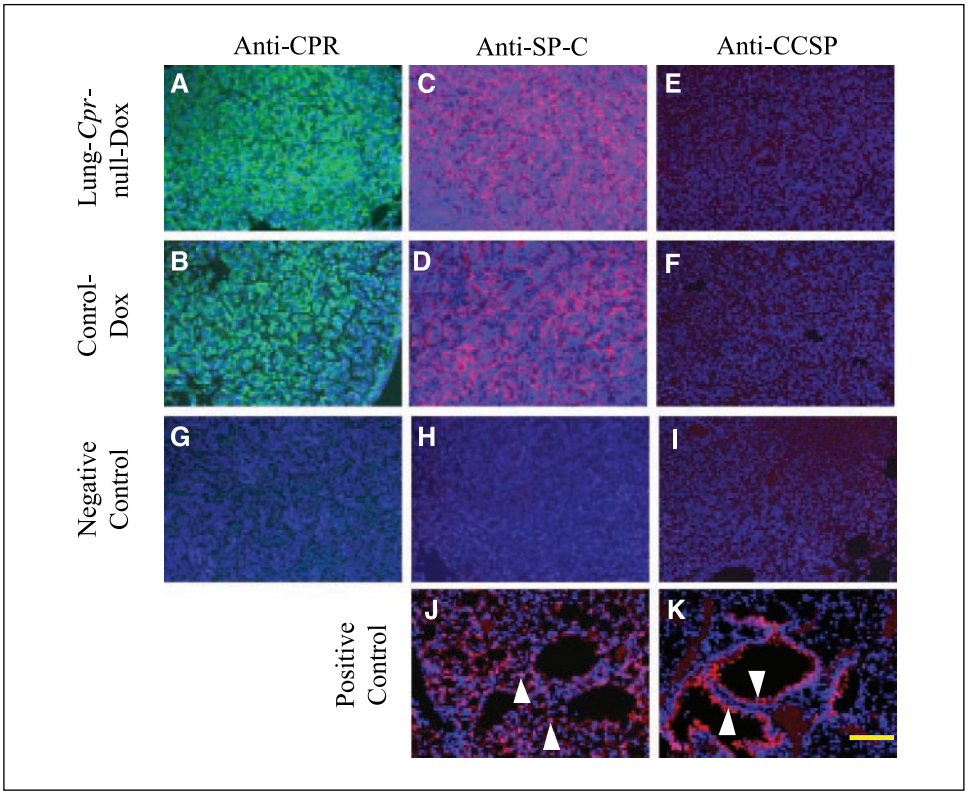

Figure 2. Immunohistochemical analysis of CPR, SP-C, and CCSP expression in NNK-induced lung tumors. Tumors from lung-*Cpr*-null-doxycycline (*A, C*, and *E*) and control-doxycycline mice (*B, D, F, G, H*, and *I*) were analyzed. Immunohistochemical analysis for CPR (*A* and *B*) was done as described in the legend of Figure 1. SP-C was detected using a rabbit anti-prosurfactant protein C antibody (*C* and *D*), whereas CCSP was detected using a rabbit anti-CCSP antibody (*E* and *F*). Alexa Fluor 594–conjugated secondary antibody was used for the detection of SP-C and CCSP, whereas Alexa Fluor 488–conjugated secondary antibody was used for the detection of CPR. The primary antibodies were omitted for negative controls (*G–I*), which were processed with either Alexa Fluor 488–conjugated (*G*) or Alexa Fluor 594–conjugated (*H* and *I*) secondary antibody. As positive controls, expression of SP-C (*J*) and CCSP (*K*) in the normal lung tissues of the control-doxycycline mouse was also examined. Bar, 50 μm. *Arrowheads,* SP-C–positive cells in the alveolar wall (*J*) and CCSP-positive cells in the airways (*K*).

Table 2. NNK-induced O^6-mG adduct formation and lung tumorigenesis in liver-*Cpr*-null mice and control littermates

A. Lung tumor multiplicity and frequency

Animals	Treatment	Tumor multiplicity (tumors/mouse)	Tumor frequency (%)
WT	Saline (n = 10)	0 ± 0	0
WT	NNK (n = 11)	6.5 ± 1.4*	100 †
Liver-*Cpr*-null	Saline (n = 13)	0.08 ± 0.08	7.7
Liver-*Cpr*-null	NNK (n = 11)	15.5 ± 2.3* ‡	100 †

B. Tissue levels of O^6-mG

Animals	O^6-mG (pmol/μmol guanine)		
	4 h	24 h	
	Lung	Lung	Liver
WT	18.4 ± 0.8	13.1 ± 0.9 (n = 3)	240 ± 20
Liver-*Cpr*-null	21.7 ± 1.9	18.4 ± 1.5§	12.9 ± 2.7§

NOTE: A. All mice were female and were treated i.p. with a single dose of NNK at 10 μmol/mouse or with 0.15 mL saline, at 2 mo of age. Thereafter, the mice were kept on AIN93G diet until they were sacrificed for tumor bioassay, at 4 mo after the NNK or saline injection. Tumor multiplicity is shown as mean ± SE. Tumor frequency was calculated as percentage of mice with tumor in each group. B. All mice (2-month-old females) were treated with a single i.p. dose of NNK at 100 mg/kg and sacrificed at either 4 or 24 h after dosing. The values shown are mean ± SE (n = 4, unless specified otherwise).
*Significantly different from corresponding saline-treated groups (P < 0.01, Mann-Whitney rank-sum test).
†Significantly different from corresponding saline-treated groups (P < 0.01, Fisher's exact test).
‡Significantly different from NNK-treated WT group (P < 0.001, t test).
§Significantly different from NNK-treated WT mice in the same column (P < 0.05, t test).

NNK-treated lung-*Cpr*-null-doxycycline mice and in selected tumors (as positive controls) from three NNK-treated control-doxycycline mice. We found that all of the tumors examined were positive for CPR (Fig. 2*A* and *B*) and SP-C expression (Fig. 2*C* and *D*), but they were negative for CCSP expression (Fig. 2*E* and *F*). In normal lung tissues, the staining for SP-C was only observed in the alveolar regions, presumably in AECII cells (Fig. 2*J*), whereas the staining for CCSP was only observed in the airway but not in the alveolar regions (Fig. 2*K*). These results indicated that the NNK-induced tumors in the lung-*Cpr*-null-doxycycline mice, as well as those in the control-doxycycline mice, were derived from CPR-expressing AECII cells.

NNK-induced O^6-mG formation in the lungs and livers of the lung-*Cpr*-null mice and control littermates. The effect of lung-specific CPR loss on NNK-induced O^6-mG formation in the lung and liver is shown in Table 1B. At 4 h after a single i.p. injection of NNK at 20 μmol/mouse, the levels of O^6-mG in the lungs of the lung-*Cpr*-null-doxycycline mice (13.1 pmol/μmol guanine) were ~37% of those in similarly treated control-doxycycline mice (35.1 pmol/μmol guanine). In a separate experiment, at 24 h after NNK injection at 200 mg/kg, a dose similar to 20 μmol/mouse for mice of 20 to 25 g body weight, the levels of O^6-mG in the lungs of the lung-*Cpr*-null-doxycycline mice (30.9 pmol/μmol guanine) were ~46% of those in the control-doxycycline mice (67.7 pmol/μmol guanine). In contrast to the significantly reduced levels of O^6-mG in the lungs of the lung-*Cpr*-null-doxycycline mice, the levels of O^6-mG in the livers of the lung-*Cpr*-null-doxycycline mice at 24 h after NNK injection were not significantly different from those of similarly treated control-doxycycline mice. No significant difference was observed between the control and control-doxycycline mice in the levels of O^6-mG in the lungs at either 4 or 24 h or in the livers at 24 h after the NNK injection (Table 1B), indicating that doxycycline had no unintended effects on the formation of O^6-mG in either the lungs or liver.

Systemic clearance of NNK and NNAL in the lung-*Cpr*-null mice and control littermates. NNAL is the major circulating metabolite of NNK in both rodents and humans (11, 30). The formation of NNAL from NNK is catalyzed by cytosolic carbonyl reductase (10), which is not CPR dependent. However, like NNK, NNAL can be bioactivated by P450 to cause lung cancers in the A/J mice (31). The results of pharmacokinetic studies confirmed that the lungs of the NNK-treated lung-*Cpr*-null-doxycycline mice were not exposed to lower doses of NNK and NNAL compared with those of the similarly treated control-doxycycline mice (Supplementary Fig. S4; Supplementary Table S4). Additionally, the plasma levels of NNK and NNAL, as well as the calculated pharmacokinetic variables (Supplementary Fig. S4; Supplementary Table S4), were not significantly different between the control and control-doxycycline groups, further indicating that doxycycline did not have a direct effect on the absorption, metabolism, or clearance of NNK and NNAL.

NNK-induced lung tumor formation in the liver-*Cpr*-null mice and WT littermates. The findings obtained using the lung-*Cpr*-null mice suggested that NNK metabolites generated in the liver do not play a major role in NNK-induced lung cancer. To confirm this hypothesis, we compared NNK-induced lung tumor formation between liver-*Cpr*-null and WT mice. Notably, a lower dose of NNK was used here because we expected the bioavailability

of NNK and NNAL to be higher in studies with the liver-*Cpr*-null mice than in the studies with the lung-*Cpr*-null mice. As shown in Table 2A, the multiplicity of lung tumors in the A/J-N_5 liver-*Cpr*-null mice (15.5 ± 2.3 tumors per mouse) was 2.4-fold higher than that in similarly treated WT littermates (6.5 ± 1.4 tumors per mouse). Tumors were not detected, or rare, in saline-treated WT or liver-*Cpr*-null mice. In the NNK-treated animals, the tumor frequency was 100% for both liver-*Cpr*-null and WT mice.

NNK-induced O^6-mG formation in the lungs and livers of the liver-*Cpr*-null mice and WT littermates. The levels of O^6-mG in the livers of the liver-*Cpr*-null mice at 24 h after a single i.p. injection of NNK at 100 mg/kg were only ~5% of those in the WT mice (Table 2B), consistent with the loss of hepatic microsomal P450 activity (8). In contrast, the levels of O^6-mG in the lungs of the liver-*Cpr*-null mice were either not significantly different (at 4 h) or else higher (at 24 h) than those of the WT mice after the NNK injection (Table 2B), indicating that the NNK-induced DNA adduct formation in the lung was not dependent on NNK metabolism in the liver.

Reduced systemic clearance of NNK and NNAL in the liver-*Cpr*-null mice. Following an i.p. injection of NNK at 100 mg/kg, the plasma levels of NNK and NNAL were significantly higher in the liver-*Cpr*-null mice than those in the WT littermates (Fig. 3). For both NNK and NNAL, $t_{1/2}$ and area under the concentration-time curve (AUC) were significantly higher, and clearance was significantly lower, in the liver-*Cpr*-null mice than in WT littermates (Table 3). For NNAL, the C_{max} value was also significantly higher in the liver-*Cpr*-null mice than in WT littermates. The pharmacokinetic data indicate that the lungs of the liver-*Cpr*-null mice were exposed to substantially higher levels of NNK and NNAL than were those of the WT mice, following the NNK injection.

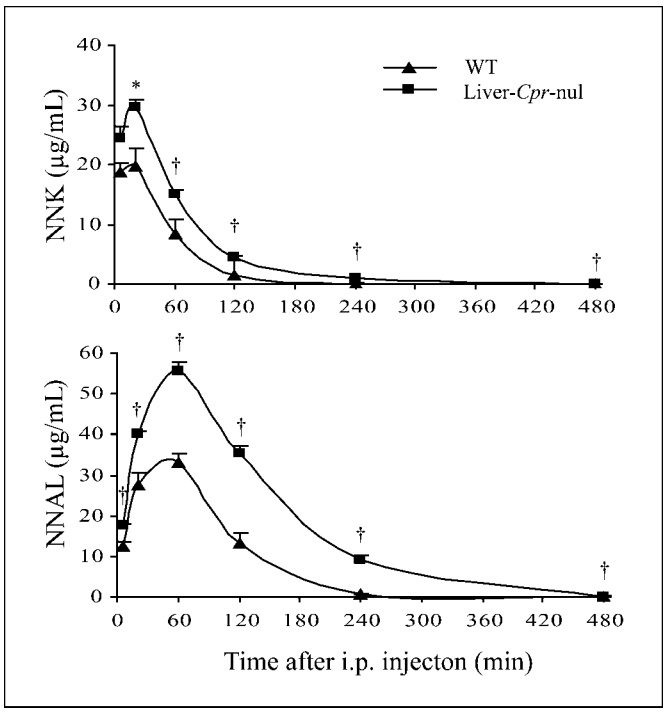

Figure 3. Plasma levels of NNK and NNAL in the liver-*Cpr*-null mice and WT littermates. All animals were 2-month-old females and were treated with a single i.p. injection of NNK at 100 mg/kg. Blood samples were collected from individual animals at six time points after the injection for determination of plasma levels of NNK and unconjugated NNAL. *Points,* mean (n = 4); *bars,* SE. *, $P < 0.05$; †, $P < 0.01$, significantly different between the liver-*Cpr*-null and WT mice, t test.

Discussion

In the lung-*Cpr*-null mouse, the deletion of the floxed *Cpr* gene required the sequential activation of two transgenes, *CCSP-rtTA* and *tetO-Cre*. Previous studies had shown that the *CCSP-rtTA/tetO* combination confers essentially lung-selective transgene expression in double transgenic mice (25, 32). The tissue specificity and developmental onset of the *Cre* gene were controlled by the rat CCSP promoter of the CCSP-rtTA transgene. The expression of rtTA in the *CCSP-rtTA* transgenic mouse was localized to subsets of Clara cells and AECII cells in the lung (21, 23), as was found here for the CRE-mediated *Cpr* deletion in the lung-*Cpr*-null mice. The *CCSP-rtTA/tetO-Cre* mice have been used by several other groups to achieve controllable deletion or activation of floxed transgenes (23, 33). Similar to the lung-*Cpr*-null mice, a mosaic pattern of doxycycline-induced deletion or activation of the floxed transgenes in the lung was reported for these transgenic mice (23, 33).

Among all of the enzymes that are CPR dependent (34), only microsomal P450 enzymes are directly associated with the clearance or bioactivation of procarcinogens and the subsequent formation of DNA adducts and initiation of carcinogenesis (10). Therefore, our findings of a decreased lung tumor multiplicity in NNK-treated lung-*Cpr*-null-doxycycline mice and an increased lung tumor multiplicity in NNK-treated liver-*Cpr*-null mice indicated that pulmonary, but not hepatic, P450-mediated bioactivation plays a major role in NNK-induced lung tumor formation. This conclusion is supported by corresponding decreases in O^6-mG levels in the lungs of the lung-*Cpr*-null-doxycycline mice, in which systemic levels of NNK and NNAL, the major circulating NNK metabolite (30, 35), as well as hepatic P450 activity in NNK bioactivation, were largely unchanged. Further support for the critical role of lung P450 in NNK-induced carcinogenesis came from studies using liver-*Cpr*-null mice, in which the levels of O^6-mG was increased in the lungs at 24 h after the NNK injection, despite a nearly total loss of hepatic P450 activity toward NNK (8). Strong support for the role of *in situ* metabolic activation in NNK-induced lung carcinogenesis was also provided by the observation that all tumors examined in the lung-*Cpr*-null-doxycycline mice originated from cells that were positive for CPR expression, indicating that cells with *Cpr* deletion and consequent loss of P450-mediated NNK bioactivation did not develop into tumors.

Our conclusion that *in situ* P450-catalyzed metabolic activation plays an essential role in NNK-induced lung carcinogenesis is consistent with the findings of several previous studies, which, based on biochemical reasoning, suggested that local generation of short-lived and highly reactive metabolites, through P450-catalyzed α-hydroxylation, is principally responsible for NNK-induced lung cancer (10, 11). NNK-induced lung tumorigenesis was inhibited by ~40% as a result of pretreatment of A/J mice with indole-3-carbinol, a treatment that led to decreased bioavailability of NNK and NNAL, presumably as a consequence of induction of hepatic P450 expression and, accordingly, decreased lung tissue levels of O^6-mG adduct (36). Indole-3-carbinol was also found to reduce the level of stable NNK metabolites in the urine of human smokers (37). A strong correlation between NNK-induced lung tumorigenesis and

Table 3. Pharmacokinetic variables for NNK and NNAL in the liver-*Cpr*-null mice and WT littermates

Animal groups	T_{max} (min)	C_{max} (μg/mL)	$t_{1/2}$ (min)	AUC (min·μg/mL)	Cl (mL/min/kg)
NNK					
WT	12.5 ± 4.3	20.2 ± 2.9	40.4 ± 0.2	1,300 ± 160	80.6 ± 10.5
Liver-*Cpr*-null	20.0 ± 0.0	29.7 ± 1.2	54.7 ± 1.9*	2,400 ± 90*	41.9 ± 1.5*
NNAL					
WT	50.0 ± 10.0	33.1 ± 2.4	47.6 ± 0.7	3,870 ± 390	26.6 ± 2.6
Liver-*Cpr*-null	60.0 ± 0.0	55.5 ± 2.5*	73.5 ± 3.2*	9,140 ± 430*	11.0 ± 0.6*

NOTE: Plasma levels of NNK and NNAL (from Fig. 3) were used to calculate the pharmacokinetic variables, including $t_{1/2}$ (half-life), T_{max} (time of peak concentration), AUC, *C*max (maximal concentration), and Cl (clearance). Values shown are mean ± SE (n = 4). Examples of the detection of plasma NNK and NNAL are shown in Supplementary Fig. S5.

*Values are significantly different between the liver-*Cpr*-null and WT mice ($P < 0.05$, t test).

the levels of lung DNA adduct formation in A/J mice (38) and F334 rats (39, 40) further supported the role of local metabolic activation in carcinogenesis. Moreover, whereas phenethyl isothiocyanate, an inhibitor of P450, and of NNK-induced lung tumor formation in animal models, reduced the levels of NNK α-hydroxylation metabolites in the lung as well as most other organs examined (41), long-term feeding of phenethyl isothiocyanate, together with NNK treatment, led to decreases in the ability of lung, but not liver, microsomes to catalyze NNK α-hydroxylation *in vitro* (42). This latter finding implicated that the protection, afforded by dietary phenethyl isothiocyanate, of animals against NNK-induced lung tumor formation was mainly mediated by selective inhibition of metabolic activation of NNK in the lung, rather than in the liver.

The present finding of a predominant role of lung P450 enzymes in NNK-induced lung tumorigenesis contrasts with our recent observation that acetaminophen-induced toxicity in mouse lung and kidney was contributed at least partly by hepatic P450-mediated metabolic activation (2). Thus, the relative contributions of the hepatic and pulmonary P450-mediated metabolic activation to xenobiotic-induced lung toxicity are compound dependent, a finding that necessitates close examination of the *in vivo* metabolism and toxicity of individual compounds.

Because microsomal CYP-mediated activities, as well as other CPR-dependent activities, are required in many endogenous metabolic pathways (34), deletion of *Cpr* could lead to disruption of cellular homeostasis and could indirectly modify the outcome of the tumor bioassay. In the current study, the rates of spontaneous formation of lung tumors were not changed in either lung-*Cpr*-null-doxycycline or liver-*Cpr*-null mice compared with the control littermates, indicating that no significant changes in lung tumor initiation or promotion occurred in these two transgenic mice, in the absence of a carcinogen. In NNK-treated mice, tumor initiation rates are expected to be altered as a consequence of P450-mediated metabolic activation. However, it is as yet impossible to directly detect whether differences exist among the experimental groups in tumor promotion following P450-mediated NNK metabolic activation. Nonetheless, the strong correlation between tumor multiplicity and tissue levels of O^6-mG, a DNA adduct formed as a consequence of P450-mediated α-hydroxylation (10), indicates that the changes in the rates of tumor formation were mainly due to a reduced metabolic activation, rather than to other, indirect factors.

The expression of rtTA in the lung was recently found to cause airspace enlargement (43, 44). In the current study, potential changes in airspace size in our lung-*Cpr*-null mouse were not investigated. However, the fact that we did not see any changes in the formation of spontaneous or NNK-induced lung tumors in *CCSP-rtTA/Cpr*$^{lox/lox}$ mice compared with *Cpr*$^{lox/lox}$ mice indicates that the expression of the rtTA transgene, and potentially any consequent effects on airspace size, did not modify NNK bioactivation or NNK-induced cancer formation in the lung.

The systemic administration of doxycycline at relatively high doses was found to cause fetoplacental toxicity (45) and alveolar simplification (46). In the present study, doxycycline was given to mice in the diet at ~1.9 mg/d/mouse, a dose that was found previously to have no effects on pregnancy or postnatal alveolarization (44). Under this low-dose doxycycline treatment protocol, we also found that the litter size was normal. Furthermore, NNK-induced pulmonary O^6-mG and lung tumor formation was not changed by doxycycline treatment in the control mice, indicating that doxycycline treatment per se did not influence the tumor outcome in the lung-*Cpr*-null mice.

In summary, our data strongly support the hypotheses that pulmonary P450 plays an important role in NNK-induced lung tumor formation by producing carcinogenic metabolites directly in the target tissue, whereas hepatic P450 plays a major role in systemic clearance of NNK, thereby protecting the lung against NNK-induced carcinogenesis. To our knowledge, this is the first *in vivo* evidence to directly show the essential role of pulmonary P450-mediated metabolic activation in NNK-induced lung cancer. Our findings suggest that, for tobacco smoke-induced lung cancer, chemopreventive strategies specifically targeting P450 enzymes in the respiratory tract should be more effective than the use of an inhibitor that also affects P450s in the liver. Our results also shed light on the importance of genetic polymorphisms of NNK-bioactivating P450 enzymes that are selectively expressed in the human respiratory tract, particularly CYP2A13 (16), in the interindividual differences in susceptibility to tobacco smoke-induced lung cancers.

The roles of pulmonary P450-mediated metabolic activation in xenobiotic-induced lung tissue toxicity and carcinogenicity are poorly understood for most, if not all, compounds. The lung-*Cpr*-null mouse model generated in this study, as well as the liver-*Cpr*-null mouse that was generated previously (8), should be broadly applicable to mechanistic studies on these additional lung toxicants.

Acknowledgments

Received 3/16/2007; revised 5/14/2007; accepted 6/4/2007.

Grant support: National Cancer Institute, NIH grant CA092596.

The costs of publication of this article were defrayed in part by the payment of page charges. This article must therefore be hereby marked *advertisement* in accordance with 18 U.S.C. Section 1734 solely to indicate this fact.

We thank Dr. Jeffrey A. Whitsett for generously providing the *CCSP-rtTA/tetO-Cre* transgenic mice, Drs. Steve S. Hecht and John R. Jalas (University of Minnesota, Minneapolis, MN) for advice on DNA adduct assays, Dr. Todd Gray for helpful discussion, Weizhu Yang and Yuan Wei for helping with breeding of transgenic mice, Helen Johnson and Fang Liu for preparation of tissue sections, Biochemistry Core, the Advanced Light Microscopy and Image Analysis Core, and the Pathology Laboratory of the Wadsworth Center.

References

1. Coon MJ. Cytochrome *P*450: nature's most versatile biological catalyst. Annu Rev Pharmacol Toxicol 2005;45:1–25.
2. Gu J, Cui H, Behr M, et al. *In vivo* mechanisms of tissue-selective drug toxicity: effects of liver-specific knockout of the NADPH-cytochrome *P*450 reductase gene on acetaminophen toxicity in kidney, lung, and nasal mucosa. Mol Pharmacol 2005;67:623–30.
3. Ding X, Kaminsky LS. Human extrahepatic cytochromes *P*450: function in xenobiotic metabolism and tissue-selective chemical toxicity in the respiratory and gastrointestinal tracts. Annu Rev Pharmacol Toxicol 2003;43:149–73.
4. Choudhary D, Jansson I, Schenkman JB, Sarfarazi M, Stoilov I. Comparative expression profiling of 40 mouse cytochrome *P*450 genes in embryonic and adult tissues. Arch Biochem Biophys 2003;414:91–100.
5. O'Leary KA, Kasper CB. Molecular basis for cell-specific regulation of the NADPH-cytochrome *P*450 oxidoreductase gene. Arch Biochem Biophys 2000;379:97–108.
6. Shen AL, O'Leary KA, Kasper CB. Association of multiple developmental defects and embryonic lethality with loss of microsomal NADPH-cytochrome *P*450 oxidoreductase. J Biol Chem 2002;277:6536–41.
7. Otto DM, Henderson CJ, Carrie D, et al. Identification of novel roles of the cytochrome *P*450 system in early embryogenesis: effects on vasculogenesis and retinoic acid homeostasis. Mol Cell Biol 2003;23:6103–16.
8. Gu J, Weng Y, Zhang QY, et al. Liver-specific deletion of the NADPH-cytochrome *P*450 reductase gene: impact on plasma cholesterol homeostasis and the function and regulation of microsomal cytochrome *P*450 and heme oxygenase. J Biol Chem 2003;278:25895–901.
9. Henderson CJ, Otto DM, Carrie D, et al. Inactivation of the hepatic cytochrome *P*450 system by conditional deletion of hepatic cytochrome *P*450 reductase. J Biol Chem 2003;278:13480–6.
10. Hecht SS. Biochemistry, biology, and carcinogenicity of tobacco-specific *N*-nitrosamines. Chem Res Toxicol 1998;11:559–603.
11. Hecht SS. Tobacco carcinogens, their biomarkers, and tobacco-induced cancer. Nat Rev Cancer 2003;3:733–44.
12. Jalas JR, McIntee EJ, Kenney PM, Upadhyaya P, Peterson LA, Hecht SS. Stereospecific deuterium substitution attenuates the tumorigenicity and metabolism of the tobacco-specific nitrosamine 4-(methylnitrosamino)-1-(3-pyridyl)-1-butanone (NNK). Chem Res Toxicol 2003;16:794–806.
13. Smith TJ, Guo ZY, Thomas PE, et al. Metabolism of 4-(methylnitrosamino)-1-(3-pyridyl)-1-butanone in mouse lung microsomes and its inhibition by isothiocyanates. Cancer Res 1990;50:6817–22.
14. Takeuchi H, Saoo K, Yokohira M, et al. Pretreatment with 8-methoxypsoralen, a potent human CYP2A6 inhibitor, strongly inhibits lung tumorigenesis induced by 4-(methylnitrosamino)-1-(3-pyridyl)-1-butanone in female A/J mice. Cancer Res 2003;63:7581–3.
15. Hecht SS, Trushin N, Rigotty J, et al. Complete inhibition of 4-(methylnitrosamino)-1-(3-pyridyl)-1-butanone-induced rat lung tumorigenesis and favorable modification of biomarkers by phenethyl isothiocyanate. Cancer Epidemiol Biomarkers Prev 1996;5:645–52.
16. Su T, Bao Z, Zhang QY, Smith TJ, Hong JY, Ding X. Human cytochrome *P*450 CYP2A13: predominant expression in the respiratory tract and its high efficiency metabolic activation of a tobacco-specific carcinogen, 4-(methylnitrosamino)-1-(3-pyridyl)-1-butanone. Cancer Res 2000;60:5074–9.
17. Su T, Ding X. Regulation of the cytochrome *P*450 2A genes. Toxicol Appl Pharmacol 2004;199:285–94.
18. Jalas JR, Hecht SS, Murphy SE. Cytochrome *P*450 enzymes as catalysts of metabolism of 4-(methylnitrosamino)-1-(3-pyridyl)-1-butanone, a tobacco specific carcinogen. Chem Res Toxicol 2005;18:95–110.
19. Hecht SS, Morse MA, Amin S, et al. Rapid single-dose model for lung tumor induction in A/J mice by 4-(methylnitrosamino)-1-(3-pyridyl)-1-butanone and the effect of diet. Carcinogenesis 1989;10:1901–4.
20. Wu L, Gu J, Weng Y, et al. Conditional knockout of the mouse NADPH-cytochrome *P*450 reductase gene. Genesis 2003;36:177–81.
21. Tichelaar JW, Lu W, Whitsett JA. Conditional expression of fibroblast growth factor-7 in the developing and mature lung. J Biol Chem 2000;275:11858–64.
22. Perl AK, Wert SE, Nagy A, Lobe CG, Whitsett JA. Early restriction of peripheral and proximal cell lineages during formation of the lung. Proc Natl Acad Sci U S A 2002;99:10482–7.
23. Perl AK, Wert SE, Loudy DE, Shan Z, Blair PA, Whitsett JA. Conditional recombination reveals distinct subsets of epithelial cells in trachea, bronchi, and alveoli. Am J Respir Cell Mol Biol 2005;33:455–62.
24. Hokuto I, Ikegami M, Yoshida M, et al. Stat-3 is required for pulmonary homeostasis during hyperoxia. J Clin Invest 2004;113:28–37.
25. Perl AK, Tichelaar JW, Whitsett JA. Conditional gene expression in the respiratory epithelium of the mouse. Transgenic Res 2002;11:21–9.
26. Markel P, Shu P, Ebeling C, et al. Theoretical and empirical issues for marker-assisted breeding of congenic mouse strains. Nat Genet 1997;17:280–4.
27. Anderson LM, Hecht SS, Dixon DE, et al. Evaluation of the transplacental tumorigenicity of the tobacco-specific carcinogen 4-(methylnitrosamino)-1-(3-pyridyl)-1-butanone in mice. Cancer Res 1989;49:3770–5.
28. Belinsky SA, Devereux TR, Foley JF, Maronpot RR, Anderson MW. Role of the alveolar type II cell in the development and progression of pulmonary tumors induced by 4-(methylnitrosamino)-1-(3-pyridyl)-1-butanone in the A/J mouse. Cancer Res 1992;52:3164–73.
29. Meuwissen R, Berns A. Mouse models for human lung cancer. Genes Dev 2005;19:643–64.
30. Adams JD, Lavoie EJ, O'Mara-Adams KJ, Hoffmann D, Carey KD, Marshall MV. Pharmacokinetics of *N*′-nitrosonornicotine and 4-(methylnitrosamino)-1-(3-pyridyl)-1-butanone in laboratory animals. Cancer Lett 1985;28:195–201.
31. Upadhyaya P, Kenney PM, Hochalter JB, Wang M, Hecht SS. Tumorigenicity and metabolism of 4-(methylnitrosamino)-1-(3-pyridyl)-1-butanol enantiomers and metabolites in the A/J mouse. Carcinogenesis 1999;20:1577–82.
32. Politi K, Zakowski MF, Fan PD, Schonfeld EA, Pao W, Varmus HE. Lung adenocarcinomas induced in mice by mutant EGF receptors found in human lung cancers respond to a tyrosine kinase inhibitor or to down-regulation of the receptors. Genes Dev 2006;20:1496–510.
33. Mucenski ML, Nation JM, Thitoff AR, et al. β-Catenin regulates differentiation of respiratory epithelial cells *in vivo*. Am J Physiol Lung Cell Mol Physiol 2005;289:L971–9.
34. Weng Y, DiRusso CC, Reilly AA, Black PN, Ding X. Hepatic gene expression changes in mouse models with liver-specific deletion or global suppression of the NADPH-cytochrome *P*450 reductase gene. Mechanistic implications for the regulation of microsomal cytochrome *P*450 and the fatty liver phenotype. J Biol Chem 2005;280:31686–98.
35. Hecht SS, Trushin N, Reid-Quinn CA, et al. Metabolism of the tobacco-specific nitrosamine 4-(methylnitrosamino)-1-(3-pyridyl)-1-butanone in the patas monkey: pharmacokinetics and characterization of glucuronide metabolites. Carcinogenesis 1993;14:229–36.
36. Morse MA, LaGreca SD, Amin SG, Chung FL. Effects of indole-3-carbinol on lung tumorigenesis and DNA methylation induced by 4-(methylnitrosamino)-1-(3-pyridyl)-1-butanone (NNK) and on the metabolism and disposition of NNK in A/J mice. Cancer Res 1990;50:2613–7.
37. Taioli E, Garbers S, Bradlow HL, Carmella SG, Akerkar S, Hecht SS. Effects of indole-3-carbinol on the metabolism of 4-(methylnitrosamino)-1-(3-pyridyl)-1-butanone in smokers. Cancer Epidemiol Biomarkers Prev 1997;6:517–22.
38. Peterson LA, Hecht SS. O^6-methylguanine is a critical determinant of 4-(methylnitrosamino)-1-(3-pyridyl)-1-butanone tumorigenesis in A/J mouse lung. Cancer Res 1991;51:5557–64.
39. Morse MA, Wang CX, Stoner GD, et al. Inhibition of 4-(methylnitrosamino)-1-(3-pyridyl)-1-butanone-induced DNA adduct formation and tumorigenicity in the lung of F344 rats by dietary phenethyl isothiocyanate. Cancer Res 1989;49:549–53.
40. Staretz ME, Foiles PG, Miglietta LM, Hecht SS. Evidence for an important role of DNA pyridyloxobutylation in rat lung carcinogenesis by 4-(methylnitrosamino)-1-(3-pyridyl)-1-butanone: effects of dose and phenethyl isothiocyanate. Cancer Res 1997;57:259–66.
41. Staretz ME, Hecht SS. Effects of phenethyl isothiocyanate on the tissue distribution of 4-(methylnitrosamino)-1-(3-pyridyl)-1-butanone and metabolites in F344 rats. Cancer Res 1995;55:5580–8.
42. Staretz ME, Koenig LA, Hecht SS. Effects of long term dietary phenethyl isothiocyanate on the microsomal metabolism of 4-(methylnitrosamino)-1-(3-pyridyl)-1-butanone and 4-(methylnitrosamino)-1-(3-pyridyl)-1-butanol in F344 rats. Carcinogenesis 1997;18:1715–22.
43. Sisson TH, Hansen JM, Shah M, et al. Expression of the reverse tetracycline-transactivator gene causes emphysema-like changes in mice. Am J Respir Cell Mol Biol 2006;34:552–60.
44. Whitsett JA, Perl AK. Conditional control of gene expression in the respiratory epithelium: A cautionary note. Am J Respir Cell Mol Biol 2006;34:519–20.
45. Moutier R, Tchang F, Caucheteux SM, Kanellopoulos-Langevin C. Placental anomalies and fetal loss in mice, after administration of doxycycline in food for tet-system activation. Transgenic Res 2003;12:369–73.
46. Hosford GE, Fang X, Olson DM. Hyperoxia decreases matrix metalloproteinase-9 and increases tissue inhibitor of matrix metalloproteinase-1 protein in the newborn rat lung: association with arrested alveolarization. Pediatric Res 2004;56:26–34.